Sun, Y.Q., Cole, Colin, Dhanasekar, Manicka, & Thambiratnam, David
(2012)
Modelling and analysis of the crush zone of a typical Australian passenger train.
Vehicle System Dynamics, *50*(7), pp. 1137-1155.

https://doi.org/10.1080/00423114.2012.656658

Modelling and Analysis of the Crush Zone of a Typical Australian Passenger Train

Y. Q. Sun[1,*], C. Cole[1,*], M. Dhanasekar[2,*] and D. P. Thambiratnam[2]

[1]Centre for Railway Engineering, CQ University, Rockhampton, QLD 4702, Australia

[2]Queensland University of Technology, Brisbane, Australia

[*]Cooperative Research Centre (CRC) for Rail Innovations, Australia

Abstract: A three-dimensional non-linear rigid body model has been developed for the investigation of the crashworthiness of a passenger train using the multi-body dynamics approach. This model refers to a typical design of passenger cars and train constructs commonly used in Australia. The high energy and low energy crush zones of the cars and the train constructs are assumed and the data explicitly provided in the paper. The crash scenario is limited to the train colliding on to a fixed barrier symmetrically. The simulations of a single car show that this initial design is only applicable for the crash speed of 35 km/h or lower. For higher speeds (e.g., 140 km/h), the crush lengths or crush forces or both the crush zone elements will have to be enlarged. It is generally better to increase the crush length than the crush force in order to retain the low levels of the longitudinal deceleration of the passenger cars.

Key words:

multi-body modelling; passenger trains; train crashworthiness; crush length; crush force

1. Introduction

Rail safety issues for passenger train vehicles around the world demand a high-energy (HE) crush or crumple zone on the train front and low-energy (LE) crush zones between vehicles to absorb the crash energy of a collision. Crush zone is the area where the structure or equipment in a vehicle is allowed to collapse and absorb the kinetic energy of an impact during the collision and reduce the kinetic energy transferred to the train driver in the cab and the passengers in each vehicle. Unfortunately, design of workable and suitable crush zones has become a great concern to the rail vehicle engineers due to the complexity of the crash event and the failure mechanisms of the HE and LE crush zones.

Modern multibody dynamics and finite element analysis methods can be used in the investigation of train collisions, crashworthiness and the absorption of energy in the structure. Analyses could range from simplified one-dimensional models used to evaluate interactions between vehicles and study the effects of varying parameters such as the crush strength to detailed three-dimensional finite element crash simulations that can be used as part of the vehicle design process [1].

Multibody dynamics formulations can be in one, two or three dimensions. The one-dimensional (1D) models consider the train to be constrained to the longitudinal track line. The two-dimensional (2D) models consider the lateral buckling of the train constructs in the investigation and the three-dimensional (3D) models consider the over-riding of vehicles in a train. Milho et al [2] presented a validated multibody model for the design of train crashworthy components. A design methodology for crashworthy structures was presented in [3]. Deterministic and evolutionary algorithms were linked with simplified models based on multibody dynamics formulations, and were used in the conceptual design to obtain the best characteristics of the crashworthy train structures. A three-dimensional collision dynamics model of a multi-level passenger train was developed to study the influence of multi-level design parameters and possible train configuration variations on the reactions of a multi-level car in a collision [4]. A collision dynamics model was used to study the kinetic and dynamic response of the individual crush zone components and the resultant car body motions prior to the tests and good agreement was obtained between the model and the test results [5]. A multi-body model was designed to carry out the crashworthiness analysis of the train-to-train collision [6] ~ [7] and used to be comparable with a 30 mph (48.3 km/h), full-scale, train-to-train crash energy management (CEM) test [8].

Where refined results are desired, finite element modelling of crash events of rail cars of performed; finite element modelling of train constructs are rare. An explicit finite element analysis of the locomotive collision was performed using ABAQUS/Explicit [9] ~ [10]. A FEA model was developed to evaluate the performance of the design of crush zone for an existing passenger rail cab car in [11, 12]. A full-rail vehicle explicit finite element model using FEA package LS-DYNA was applied to carry out the train crashworthiness analysis [13-17]. A three-dimensional FE model was developed to evaluate the train crashworthiness [18]. In [19, 20], the nonlinear finite elements were integrated with conventional rigid or flexible multibody descriptions in order to build better general vehicle models to investigate the vehicle crashworthiness.

Differing from the most 3-dimensional modelling reviewed above, this paper reports the detailed multi-body dynamics modelling method of a three-dimensional passenger train developed for crashworthiness analysis of a typical Australian passenger car and train constructs. Each passenger car is analysed as a fully detailed multi-body dynamics model with the non-linear springs and dampers representing the secondary and primary suspensions that are used to connect the car body, bogie frames and wheelsets, and more importantly the detailed non-linear wheel-rail contacts are taken into account. Therefore, the train lateral and vertical dynamics can be realised besides train longitudinal dynamics, so that, train derailment can be investigated due to collisions. The non-linear springs representing the couplers are used for the connection of vehicles. The most common train crash scenario, namely collision with a fixed barrier is used in the analysis of the train crashworthiness. Since the Australian rail industry operates trains under the speed of 160 km/h, the analyses were limited to crash speed in the range of 35 ~ 170 km/h with particular focus on the design of crush zones. Furthermore, the effects of the characteristics of crush zone (crash force and crush length) to the design of crush zones has been investigated.

2. Frontal Collision of Rail Vehicles

Frontal collision of rail vehicles can potentially cause serious injuries, in some cases fatalities, to the drivers and passengers of the train. To minimise the seriousness of the frontal collision, each vehicle, especially the frontal locomotive, must have an adequate structural system in terms of strength to withstand the forces of collision as well as deformation capability to ensure survival space for all occupants. The train construct must also possess appropriate total crash energy management system comprising of deformable crush elements and push back couplers.

2.1. Frontal Collision

Three dominant modes of train collisions can be observed from the analysis of the Australian rolling stock crash accidents [21]. These are: (1) frontal; (2) rear; and (3) side collisions. Of them, the frontal collision appears to represent the greatest threat to both the train drivers and the passengers. Many train accidents at level crossings or the rear-end collisions in which a lead locomotive is involved also challenge the train frontal crashworthiness but less seriously than the frontal impacts due to head-on collisions or collisions with a fixed barrier. Therefore, many frontal crash scenarios have been selected to evaluate the crashworthiness of the rail vehicles and that of the train constructs. With a view to ensuing safety, many standards emphasise on the seriousness of the frontal collision with clear direction towards protection against the head-on crashes. For example, in the current Australian standard for crashworthiness [22], rail vehicles are to be designed assuming several longitudinal impact scenarios commencing at 10km/h travel with increments of 3km/h until the frontal impact force (coupler force) reaches 5500kN or the speed reaches a maximum value of 20 km/h.

2.2. Energy Dissipation Mechanisms

The crash energy dissipation mechanisms for a passenger train should be properly designed to satisfy the requirements of the structural crashworthiness of a train construct to perform in an appropriate manner for a set of prescribed crash scenarios, mostly based on frontal collisions. The energy dissipation mechanisms that incorporate various structural design features and special equipment can be used to absorb the crash energy in a controlled manner without interfering with the survival spaces of the drivers and the passengers and without compromising the minimum decelerations for the safety of the occupants.

Through appropriate design, localised large deformation of the crush zones at selected locations can be minimised whilst maintaining maximum energy absorption. The majority of the crash energy absorption takes place at the front of the train; therefore, the crush zone at the front of the train is usually called the high energy (HE) crush zone. The absorption of remaining energy and the subsequent impact energy between passenger cars happen at the coupler locations, where there are also specifically designed energy absorbing crush elements, which are called the low energy (LE) crush zones. Both the HE and the LE crash zones can take the form of one or a combination of sequential crushable elements such as the push-back coupler, the buffers made up of tubes or honeycomb, and parts of the structure itself.

The HE and LE crush zones ensure occurring of crushing progressively. Idealised curve of force-crush characteristic for a crush zone is like a flight of stairs, as shown in Fig. 4 (a) with triple-tiered characteristic. With such arrangements and the characteristics of HE and LE crush zones, passenger cars can distribute the collision energy in such a way that the integrity of the occupant areas is maintained through appropriate collision energy management. Such design of HE and LE crush zones extends from the conventional crashworthiness design practice. Collision performance of conventional design typically concentrates crush at the front of the leading passenger car in which there is little resistance to deformation of the occupant areas once the peak load is exceeded. The difference between the HE and LE crush zone design and the conventional one is that the passenger cars with the design of the HE and LE crush zones can more efficiently absorb collision energy and transfer the crash energy to the following cars rather than being concentrated entirely on the leading car. This dissipation is accomplished by the controlled crush of three components: (1) the push-back coupler, (2) the buffers made up of tubes or honeycomb, and (3) parts of the structure itself. Due to the different roles of the HE and LE crush zones, their characteristic parameters, even for the LE crush zone in different location, should be designed differently for a certain crash scenario, which can be achieved through a optimisation method [24]. However, in the case study in this paper, the parameters for the structure absorbers in both the HE and LE crush zones are considered to be the same.

2.3. Collision Forces

In crash scenarios of frontal collisions, the longitudinal force is an important factor to assess the severity of the crash. Traditionally the longitudinal forces have been specified as proof loads to ensure that car body frame can transmit operational compressive loads and that the spaces where the drivers and the passengers occupy retain their integrity. For example, the requirement of longitudinal loading due to frontal collisions is specified by the Transport Safety Investigation (TSI), UK [23] as 1.5MN higher than the mean collapse load of the designated crush zones. Stronger survival cells for driver and passengers appear highly desirable, and will undoubtedly influence safety standards. However, the fact that the increase in strength generally might increase the weight, and hence the collision energy is an issue the current crashworthiness design should accommodate. Although stiffer lightweight materials are available in the market, they are not considered as part of the investigation contained in the paper with a view to keeping the costs low.

2.4. Rail Vehicle Response

In a frontal crash between two passenger trains or between a passenger train and a fixed barrier, severe dynamic interactions occur sequentially. The rail vehicle dynamic response during a collision is significantly influenced by the interactions of the colliding vehicles, the nature of the coupling between the vehicles, and the designated crush zone performances. Even in a train collision with initially in-line and coincident centrelines, the front vehicle may vertically override its counterpart or the trains may undergo lateral buckling due to dynamic interactions between vehicles. The couplers between vehicles can greatly contribute to train lateral buckling as a consequence of collision. When a high longitudinal load is present, the connection formed by the couplers would laterally push on the ends of the vehicles, with only a small perturbation. As a result, two adjacent vehicles will be laterally offset from each other leading to a sawtooth pattern of the train construct. At extreme, lateral buckling can cause train derailment. Overriding vehicles during train derailment are often associated with substantial loss of occupant space and consequent casualty. The tendency to override or lateral buckling depends upon the nature of the collision forces and the dynamic responses of the vehicles in a train to the impact force, as well as the initial conditions of the impact.

3. Modelling of Single Rail Vehicle Collision

3.1. Modeling of Components

The model of a single passenger car and its bogies are shown in Fig. 1 (a) and (b) respectively.

Vehicle model

Both components of the car body and the bogie frames are modelled as single mass with 6 degrees of freedom (DOF) – longitudinal, lateral and vertical translations, and roll, pitch and yaw rotations about X, Y and Z axes. The connections (the secondary suspensions) between the car body and the bogie frame include:

- Two vertical coil spring elements,
- One spring element for the anti-roll bar, and one spring element and one damper with series flexibility for the traction rod in the direction specified by the attachment points of the coupling,
- One lateral and two vertical bumpstops, two vertical viscous dampers, and two lateral viscous dampers and two yaw dampers with series flexibility in the direction specified by the coupling's attachment points respectively.

The wheelset is modelled as a single mass with 5 degrees of freedom (the pitch rotation is disregarded). The connections (the primary suspensions) among one bogie frame and two wheelsets include:

- 12 spring and damping elements in the three X, Y and Z directions,
- Two lateral and four vertical bumpstops, and four vertical viscous dampers in the direction specified by the coupling's attachment points.

The basic parameters of a passenger car is given in Appendix – I. The model is established in Gensys.

Wheel – rail contact model

The wheel and rail profiles shown in Fig. 2 are chosen for the modelling of the contact characteristics. Instead of the consideration of one or two wheel-rail contact points, three different wheel-rail contact points can be in contact simultaneously and are considered in the wheel-rail modelling. Through three spring elements normal to three wheel-rail contact points, the normal wheel-rail contact forces are determined. The calculations of tangent creep forces at three wheel-rail contact surfaces are made in a lookup table calculated using Kalkar creep theory.

Track model

The rail is modeled as a massless block under a wheel (Fig. 1 (b)). The rail is connected to the track via lateral and vertical springs and dampers. The track is modeled as a mass block (Fig. 1 (b)) under a wheelset. The track is allowed to have translations in the lateral and the vertical directions and rotation about the longitudinal direction. The connections between the track and the ground include:

- Two vertical coil spring elements,
- Two vertical dampers with series flexibility and one lateral damper with series flexibility.

3.2. Modeling of Crush Zones

In Fig. 3, the indeformable space of vehicle car body, which is assumed as the passenger area, is modelled as a rigid body and a single mass with 6 degrees of freedom. The components of the crush zones – push back coupler, buffers and structure energy absorbers are modelled as massless. The barrier is modelled as a fixed rigid body. Generally, the crush zones are designed to absorb the impact energy during the collision via the plastic compression deformation. The design of crush zones, which are supposed to absorb the entire impact energy without affecting the nondeformable space of car body, depends on many factors such as the vehicle crash speed, the weight and number of vehicles in a train and crush zone's crush force and length characteristics. In this paper, the initial idealised crush zone's crush force and length characteristics for the HE and LE zones are chosen as shown in Fig. 4. If the nondeformable space is affected, a mechanical stop with quite a large stiffness (e.g. 50MN/m) is assumed.

The components of the HE and LE zones include one push back coupler, two buffers (no buffers in the LE zone) and the structure energy absorbers. Their crush lengths are taken as 300mm for the push back coupler, 400mm for the buffers and 400mm for the structure energy absorbers.

The push back coupler or the buffer or the structure energy absorbers can be modelled as an element with a spring (k) in series with a friction block (F_f) and in parallel with a damper (c) in the longitudinal direction, as shown in Fig. 5. A crush zone comprises of a series of these elements.

In Fig. 5, the spring with stiffness coefficient k is serially coupled with the friction block with sliding force F_f, which means that the coupling force through the element is the same for the spring part as in the friction part. If the deformations of the ends of the element are smaller than F_f/k, no sliding motion is assumed to take place in the friction block; instead all motion will take place elastically in the spring part. If the deformation of the element exceeds F_f/k, the friction block will move the stretch required to ensure that the force over the spring part does not exceed the force F_f. In the initial idealised HE crush zone's force-crush characteristics shown in Fig. 4 (a), F_f equal to 2000 kN, 3500 kN and 4000 kN is selected for the push back coupler, the buffer and the structure energy absorbers respectively with referring to [3] and [5]. If k is selected to be 500,000 kN/m (It is thought the selection of k = 500,000 kN/m is reasonable with the author's experience) and at the beginning of train collision with the barrier, the end of push back coupler at first touches the barrier and then is compressed. When its compression is 4mm (F_f/k = 2000/500000), the friction block will move the required stretch of 300mm while the force at the end will not exceed 2000 kN. When the plastic deformation of push back coupler is fully consumed, the crash force is then transferred to the buffer. When its compression is 7mm (F_f/k = 3500/500000), the plastic deformation of buffer will begin until moving 400mm while the force will be equal to 3500 kN. The crash force is finally transferred to the structure absorber. When its compression is 8mm (F_f/k = 4000/500000), the plastic deformation of the structure absorber begins until moving 400mm while the force is equal to 4000 kN. The occupant areas begin to be challenged when all the CEM force characteristics are exceeded. The damper in Fig. 5 represents the internal damping of the metal and a small value (0.2 kN/(m/s)) is chosen for this purpose. In addition, a two-dimensional friction block is used to present the friction between the end of this element and the surface of the barrier.

3.3. Solution Technique

Several integration methods are available in Gensys. The two step Runge-Kutta method with step size control is selected for the simulations. The integrator has variable time steps between the selected maximum of 1 millisecond and minimum of 1 microsecond to ensure the numerical stability, and the length of the step is calculated based on how fast the error increases or decreases between two consecutive time steps.

3.4 Validation of the Simulation

The simulation model has been validated using a FE modelling results of Xue et al. [24]. The FEA modelling for a passenger vehicle is shown in Fig. 6, which is similar to a type of vehicle running in Australia. Its basic data are given in Table 1 and the corresponding Gensys modelling is shown in Fig. 7. Based on [24], the idealised characteristic of crush zone – crush force verse crush length is given in Fig. 8. The average force over the whole period is 3.5MN. The longitudinal displacement at Node 48298 in Fig. 7 [24] is taken to compare the result from Gensys modelling, shown in Fig. 9. The maximum displacement from Gensys modelling is 3220.7 mm and the value from [24] is 3075 mm. The error is 4.5%, which is quite reasonable.

3.5 Results & Discussions

The crashworthiness of one single car colliding symmetrically on a fixed rigid barrier as shown in Fig. 7 is first considered for simplicity. One single passenger car is assumed to collide on the fixed barrier at different crash speeds after 0.1s (sufficient to achieve steady state and numerical stability) from the beginning of simulation to examine the initial design of HE crush zone.

Some simulation results for the single car at the speeds of 25 km/h, 37.8 km/h and 50 km/h are shown in Fig. 10, including the frontal impact forces, car body's longitudinal displacements, velocities and accelerations, the vertical friction force on the crash surface and the normal wheel-rail contact forces.

It is found from Fig. 10 (a) that at the crash speed of 37.8 km/h, the initial design of HE crush zone absorbs the whole crash energy. It is expected that at speeds lower than this, the crush zone can absorb the whole crash energy. It is also noticed that the structure energy absorber is not activated even at the speed of 25 km/h. However, for the 50 km/h case, the energy absorbers in the HE crush zone are totally consumed, and the structure, which is required to be nondeformable, is hit with quite a large impact force, for example, reaching about 32,000 kN at the speed of 50 km/h.

From Fig. 10 (b), it is obvious that the higher the speed, the larger the maximum longitudinal displacement. For crash speeds at or lower than 37.8 km/h, the car body's longitudinal velocities after collision are close to zero, and almost the same. However, for the higher crash speed, the car body bounces back at a steady velocity, e.g., at the crash speed of 50 km/h, the velocity for bouncing back is -5 m/s. The presence of crush zone can significantly reduce the car body's longitudinal deceleration, keeping it within the level of 6.4 g. Once the crush zone is used up, the deceleration will increase dramatically due to the impact to the nondeformable structure, for example, the maximum deceleration is about 58g at the crash speed of 50 km/h based on Fig. 10 (c).

Due to the symmetric collision, the lateral friction force between the car body front and the barrier surface is very small and near to zero, which is not shown and discussed in this paper. However, the vertical friction force is large enough due to the location of HE crush zone lower than level of car body mass centre. The upper graph in Fig. 10 (d) shows the vertical friction force at the crash speed of 37.8 km/h. Because the positive direction is downward, the first peak force plus the longitudinal frontal impact force will make the car body have a clockwise pitch rotation. The pitch rotation of car body can significantly affect the wheel-rail normal contact forces. The lower graph in Fig. 10 (d) shows these contact forces. The wheel-rail normal contact force on the first wheelset is increased to 148.5 kN from the static wheel load of 76 kN while the force on the fourth wheelset is dramatically decreased, reaching to zero for a short period. This means that the fourth wheelset loses the contact with the rail and the wheel unloading reaches zero.

4. Modeling of Rail Vehicle Construct (Train)

Based on the modelling of the single passenger car, a passenger train construct comprising of several passenger cars was generated using Gensys software.

4.1 Number of Vehicles

In this paper, train models with four, seven and ten cars have been considered. The first car is the motored passenger car and the rest are the trailing passenger cars. The two cars have the same shape and size, with the difference being that the motored car has the heavier bogie frames and wheelsets. For where the coupler is in tension, it is modelled as a linear spring with stiffness coefficient of 20 MN/m; if it is in compression, it is modelled as a push back coupler with the characteristics shown in Fig. 4 (b). Fig. 11 shows these train models. The effect of the number of vehicles on the collision simulations on the fixed barrier have been discussed in [25] by the authors. Generally, the first peak of frontal impact force is only affected by 1^{st} to 3^{rd} vehicles. If the maximum dynamic responses of the first vehicle and the first coupler are the main concern, then the train model with four vehicles gives adequate data for crush zone analysis.

4.2 Effect of Speed of Travel

The train model with 4 cars is selected to carry out the simulations on the effect of speed to train crashworthiness. Fig. 12 shows some selected simulation results at the crash speeds of 35, 70, 105, 140 and 170 km/h; the frontal impact forces, the accelerations at the first car body mass centre, the first coupler forces, and their absolute maximum values versus speeds are presented and discussed.

The frontal impact force, the first coupler force and the accelerations significantly change with the increase in crash speed as shown in Fig. 12 (a), (b) and (c) respectively. In the situation of single car simulation at the speed of 35 km/h, the crash energy was totally absorbed by the HE crush zone (refer to Fig. 10 (a)). From Fig. 12 (a), however, the train model with four car units, the HE zone has not absorbed the whole of crash energy at that speed due to a series of consequent impacts among the passenger cars. It can be seen from Fig. 12 (d) that beyond the speed of 70 km/h, both the maximum frontal impact forces and the maximum acceleration change almost in positive linear proportion with the speeds, with the increase of about the same 150% for the frontal impact force and the acceleration respectively with the speed increase of 143% from 70 km/h to 170 km/h. However, when the speed increased by 100% (from 35 km/h to 70 km/h), both the maximum frontal impact force and the maximum acceleration have increased by about 185%. It is obvious that the initial design of crush zone has a significant effect at the low speed crashes (e.g. 35 km/h). For the crashes with the speeds higher than 70 km/h, the effect of initial design of crush zone is very limited and the different design of crush zone with higher strength is accommodated.

5 Parametric Studies on Crush Zone Designs

Based on the simulations presented in Section 4, for higher collision speeds the structure must be stronger in the design of crush zone. In this section, the two characteristic parameters – crush force and crush length are examined for the design of crush zone at the high speed. Two speeds of 70 and 170 km/h were selected for the simulations. Only the parameters of the absorbers of the structure, in both the high and the low energy crush zones, are selected to be changed by the same amount. Fig. 13 shows the frontal impact forces and the accelerations of the first car body mass centre under the conditions of the structure absorber's force being increased from 4000 kN to 8000 kN, 16000 kN, 32000 kN and 40000 kN respectively with the original absorber structure length remaining unchanged.

From Fig. 13 (a), it can be observed that the design of the high crush zone is not adequate to totally absorb the crash energy by increasing the absorber's crush force alone. When the absorber structure's crush force is increased to 40000 kN, the high crush zone absorbs the crash energy, but the frontal impact force level is higher and the maximum deceleration is also much higher, being over 100 g as shown in Fig. 13 (b). However, among these limited cases of the simulations, the absorber structure's crush force of 16000 kN gives the lowest levels of both maximum frontal impact force and maximum deceleration. It is apparent that the absorber structure with the crush force of 16000 kN is selected for the investigation of the effect of the crush length to the train crashworthiness at the speed of 70 km/h. Fig. 14 shows the frontal impact forces and the accelerations of the first car body mass centre under the conditions of the structure absorber length being increased by 0.5, 1.0, 1.5 and 2.0m respectively with the structure absorber force of 16000 kN remaining unchanged.

From Fig. 14 (a), it can be observed that the peak force is not so significantly reduced by increasing the crush length from 0.5 m to 1.5 m. Until the crush length is increased to 2.0 m, the crash energy is completely absorbed by the HE crush zone.

It is interesting to notice that the maximum deceleration before the time of 0.2 s, which is about -30 g, is almost the same for all cases. It can be seen that after the absorber structure's crush length is increased by 1.0 m, it is not significant to further increase it in terms of the maximum deceleration because it requires almost the same.

Simulations have also been carried out for the higher speed of 140 km/h using the same model as the previous one and some results are shown in Fig. 15. From Fig. 15 (a), it can be observed that the simulations on the effect of the selected absorber structure'a crush forces to the train crashworthiness show that when the crush force is 32000 kN, the frontal impact force is the smallest among the selected cases. Based on this fact, the simulations on the effect of the selected absorber structure's crush lengths to the train crashworthiness are carried out and the frontal impact forces are shown in Fig. 15 (b). It can be seen that when the absorber structure's crush length is increased by over 4.5 m, the crush energy might be totally absorbed by the HE crush zone.

6 Conclusions

A multi-body dynamics formulation of a three-dimensional passenger train model has been described for the vehicle and train crashworthiness analyses. The design of the HE and LE crush zones are particularly focussed.

The simulations of the single vehicle longitudinally colliding with a fixed barrier show that the typical designs considered are only limited to the crash speeds less than 35 km/h. For the higher speeds, the HE crush zone has to be structurally improved through either by increasing the lengths of crush zone elements or increasing the forces of crush zone elements. The simulations show that the outcome of increasing the length of crush element is better than that of increasing the force of crush element because the maximum deceleration can be reduced more significantly. However, due to the limitation of rail vehicle size, the length of crush element cannot be increased too much, so the design of length and force of crush element has to be traded off.

From the simulation of train crash for a higher speed (e.g. 70 km/h), the level of the maximum deceleration of car body mass centre mostly depends on the force of crush element in the HE crush zone. When the length of crush element is so increased that the crash energy is completely absorbed by the HE crush zone, the maximum deceleration is not reduced.

The design of crush zones in a passenger train should be realised using an optimization method. The method can be implemented in the three-dimensional passenger train model proposed in this paper so that the optimum design of crush zones with the constraints of dimension of crush element and maximum deceleration of car body can be obtained.

Acknowledgments

Rail CRC Innovation Australia financially supported this research to the third author via a Rail CRC project R3.114. The support, involvement and encouragement of the colleagues of the Centre for Railway Engineering, CQUniversity and the fellows of Queensland University of Technology are thankfully acknowledged.

References

[1]. S W Kirkpatrick, M Schroeder and J W Simons, 2001. Evaluation of Passenger Rail Vehicle Crashworthiness. International Journal of Crashworthiness, Vol. 6, No. 1, pp. 95-106.

[2]. Milho, J. F., Ambrósio, J. A. C. and Pereira, M. F. O. S., 2003. Validated multibody model for train crash analysis. International Journal of Crashworthiness, Vol. 8, No. 4, pp. 339–352

[3]. Dias, J. P. and Pereira, M. S., 2004. Optimization methods for crashworthiness design using multibody models. Computers and Structures, Vol. 82, pp. 1371–1380

[4]. Priante, M., Tyrell, D. and Perlman, B., 2006. A Collision Dynamics Model of a Multi-Level Train. Proceedings of IMECE2006 – ASME International Mechanical Engineering Congress and Exposition, November 5-10, Chicago, Illinois, USA.

[5]. Jacobsen, K., Tyrell, D. and Perlman, B., 2004. Impact Tests of Crash Energy Management Passenger Rail Cars: Analysis and Structural Measurements. Proceedings of ASME RTD2004: ASME International Mechanical Engineering Congress, November 13-19, Anaheim, CA, USA.

[6]. Parent, D., Tyrell, D. and Perlman, A. B., 2004. Crashworthiness Analysis of the Placentia, CA Rail Collision. International Crashworthiness Conference, July 14-16, San Francisco, California, USA.

[7]. Mallon, P., Perlman, B. and Tyrell, D., 2008. The Influence of Manufacturing Variations on A Crash Energy Management System. Proceedings of ASME Rail Transportation Division Fall Technical Conference, September 24-25, Chicago, Illinois, USA

[8]. Priante, M. and Martinez, E., 2007. Crash Energy Management Crush Zone Designs: Features, Functions, and Forms. Proceedings of ASME/IEEE Joint Rail Conference & Internal Combustion Engine Spring Technical Conference, March 13-16, Pueblo, Colorado, USA.

[9]. Tyrell, D., Severson, K., Marquis, B., Martinez, E., Mayville, R., Rancatore, R., Stringfellow, R., Hammond, R. and Perlman, A. B., 1999. Locomotive Crashworthiness Design Modifications Study. Proceedings of the 1999 IEEE/ASME Joint Railroad Conference, April 13-15, USA.

[10]. Stringfellow, R., Rancatore, R., Llana P. and Mayville, R., 2004. Analysis of Colliding Vehicle Interactions for The Passenger Rail Train-to-Train Impact Test. Proceedings of JRC2004: ASME/IEEE Joint Rail Conference, April 6-8, Baltimore, Maryland, USA.

[11]. Martinez, E., Tyrell, D., Rancatore, R., Stringfellow, R., Amar, G., 2005. A Crush Zone Design for An Existing Passenger Rail Cab Car. Proceedings of ASME International Mechanical Engineering Congress & Exposition, November 5-11, Orlando, Florida, USA

[12]. Priante, M., Tyrell, D. and Perlman, B., 2005. The Influence of Train Type, Car Weight, and Train Length on Passenger Train Crashworthiness. Proceedings of JRC2005 Joint Rail Conference, March 16-18, Pueblo, Colorado, USA.

[13]. Kirkpatrick, S. W. and MacNeill, R. A., 2002. Development Of A Computer Model For Prediction Of Collision Response Of A Railroad Passenger Car. Proceedings of: JRC2002 ASME/IEEE Joint Rail Conference, April 23-25, Washington D.C., USA.

[14]. Xue, X. and Schmid, F. Modelling Study to Validate Finite Element Simulation of Railway Vehicle Behaviour in Collisions. Proceedings of 5th European LS-DYNA Users Conference.

[15]. Xue, X., Schmid, F. and Smith, R. A., 2007. Analysis of the structural characteristics of an intermediate rail vehicle and their effect on vehicle crash performance. Proc. IMechE, Vol. 221, Part F: J. Rail and Rapid Transit, pp. 339-352.

[16]. Anghileri, M., Castelletti, L. M. L., Pirola, M., Pistochini, F. and Raiti, S., 2008. C IV class tram crashworthiness assessment. International Journal of Crashworthiness, Vol. 13, No. 4, pp. 425–435

[17]. Gao, G. J., and Tian, H. Q., 2007. Train's crashworthiness design and collision analysis. International Journal of Crashworthiness, Vol. 12, No. 1, pp. 21–28.

[18]. Ujita, Y., Funatsu K. and Suzuki, Y., 2003. Crashworthiness investigation of Railway Carriage. QR of RTRI, Vol. 44, No. 1, pp. 28-33.

[19]. AMBRÓSIO, J., 2005. Crash analysis and dynamical behaviour of light road and rail vehicles. Vehicle System Dynamics, Vol. 43, No. 6–7, pp, 385–411

[20]. PEREIRA, M. S., AMBROSIO J. A. C. and DIAS, J. P., 1997. Crashworthiness Analysis and Design Using Rigid-Flexible Multibody Dynamics with Application to Train Vehicles. International Journal for Numerical Methods in Engineering, Vol. 40, pp. 655-687.

[21]. G. Michal, W. Li, K. Tieu and R. Dwight, 2010, CRC R3.114: Accidents Analysis based on ATSB's reports for the 1997-2010 period - Rev.0.2, October 8, 2010

[22]. Australian RISSB, 2008 Railway Rolling Stock - Body Structural Requirements: Locomotive Rolling Stock, RDS 7520 - Part 1, Freight Rolling Stock, RDS 7520 - Part 2, Passenger Rolling Stock, RDS 7520 - Part 3.

[23]. A. ERSKINE, 2003. STRUCTURAL CRASHWORTHINESS LITERATURE SEARCH. Rail Safety and Standards Board, UK, REPORT NO. : ITLR-T12004-001.

[24]. X. Xue; R. A. Smith; F. Schmid, 2005. Analysis of crush behaviours of a rail cab car and structural modifications for improved crashworthiness. International Journal of Crashworthiness, Vol. 10, No. 2, pp.125–136.

[25]. Sun, Y. Q., Cole, C. and Dhanasekar, M., 2011. Multi-body Modelling of Wagon Train for Crashworthiness Analysis. Proceedings of 22nd International Symposium on Dynamics of Vehicle on Roads and Tracks, Aug. 15th ~ 19th, Manchester, UK.

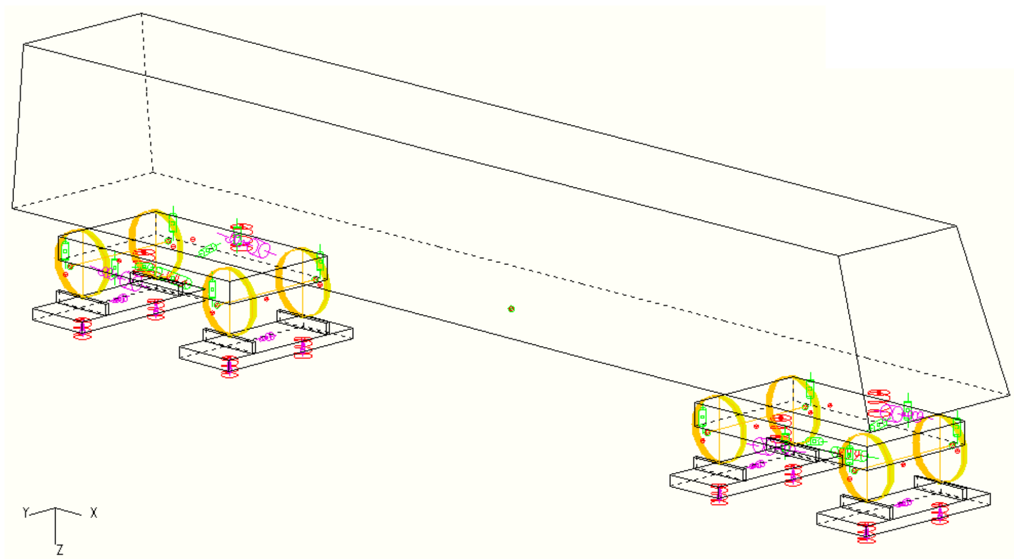

(a) Passenger Car

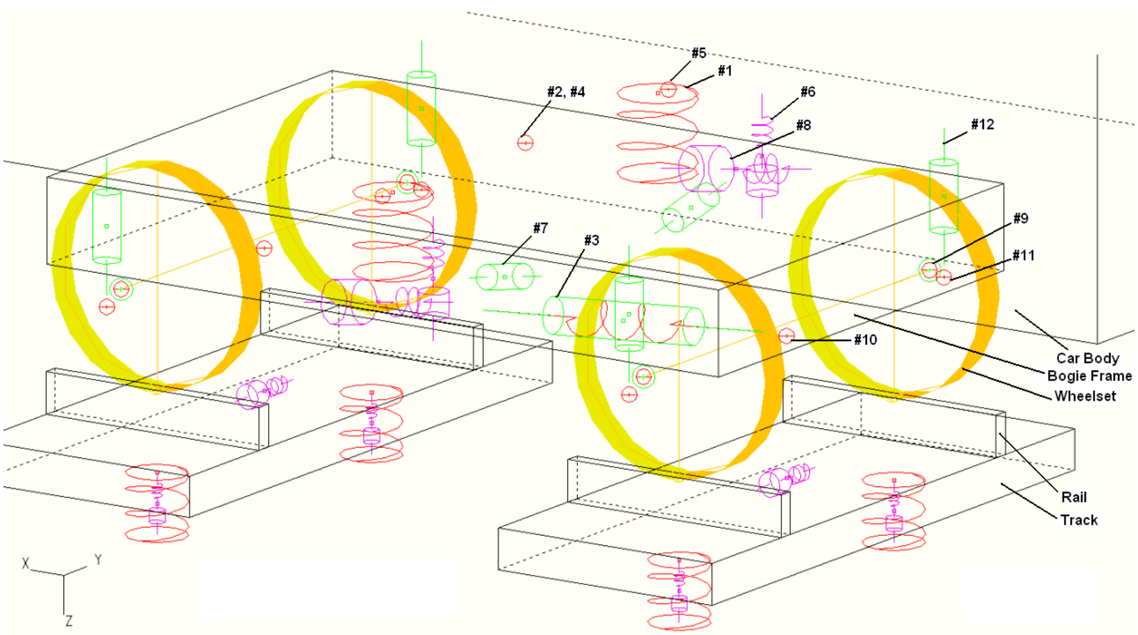

(b) Passenger Car Bogie (the secondary suspensions: #1 –2 coil springs, #2 – anti-roll bar, #3 – traction rod, #4 – 1 lateral bumpstop, #5 – 2 vertical bumpstops, #6 – 2 vertical viscous dampers, #7 – 2 lateral viscous dampers, and #8 – 2 yaw dampers; the primary suspensions: #9 – 3×4 springs, #10 – 1×2 lateral bumpstop, #11 – 2×2 vertical bumpstops, and #12 – 1×4 vertical viscous dampers)

Fig. 1 Passenger Car Model

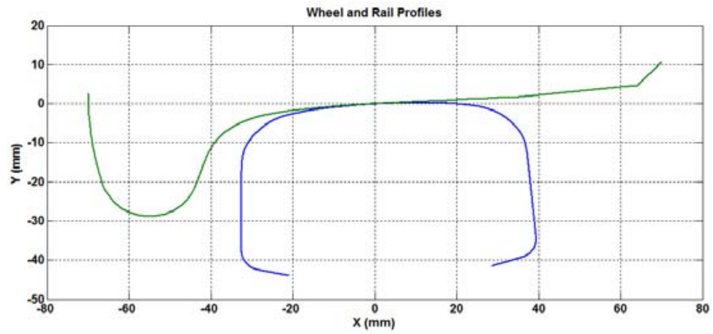

Fig. 2 Wheel and Rail Profiles

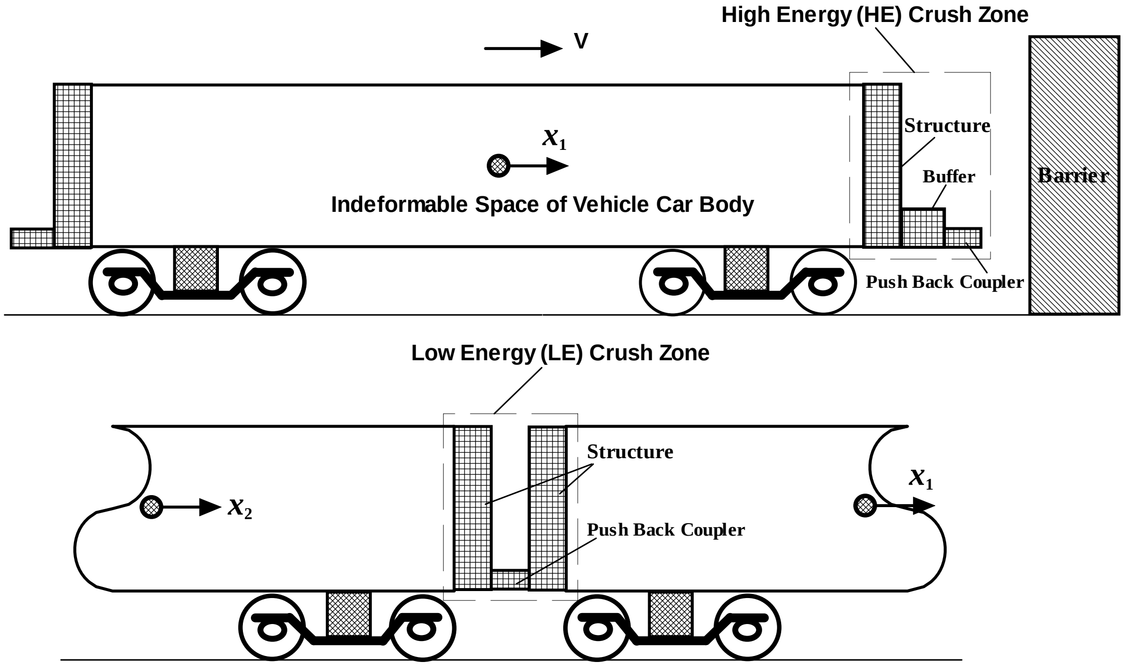

Fig. 3 Crush Zone Modelling

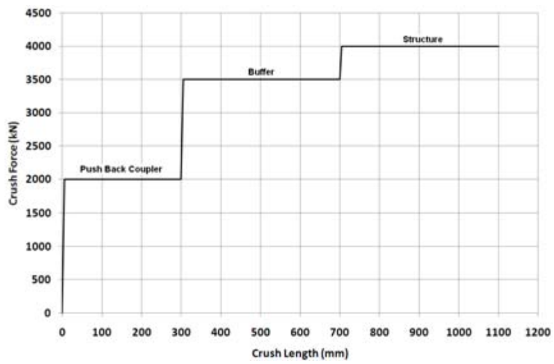

(a) HE Zone

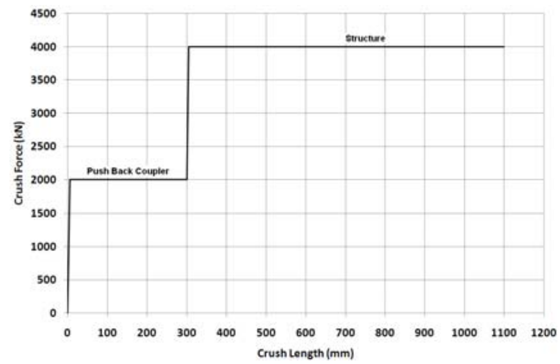

(b) LE Zone

Fig. 4 Idealised Crush Zone's Force and Crush Length Characteristics

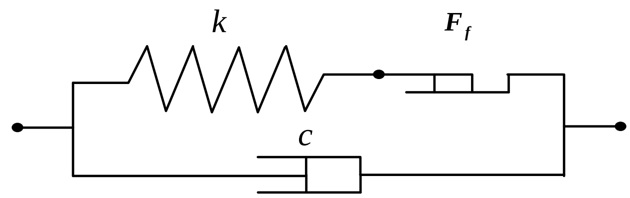

Fig. 5 Energy Absorber Modelling

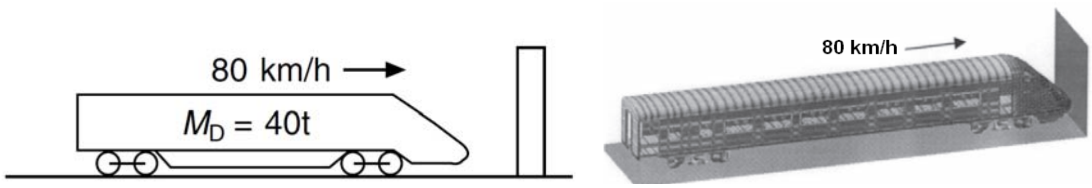

Fig. 6 FEA Modelling [24]

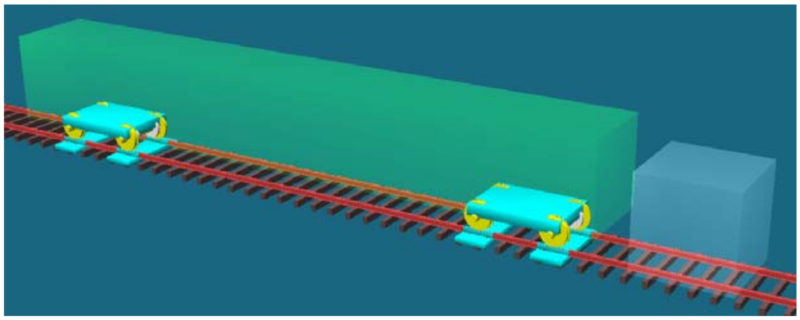

Fig. 7 Modelling of Single Car Collision

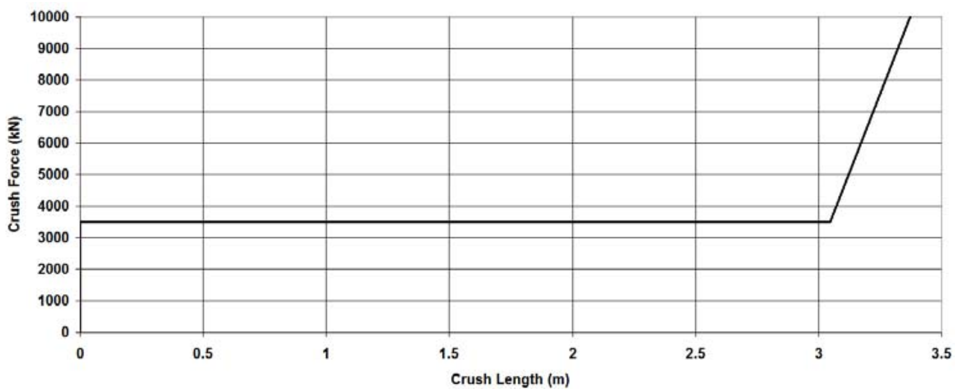

Fig. 8 Idealised Characteristics

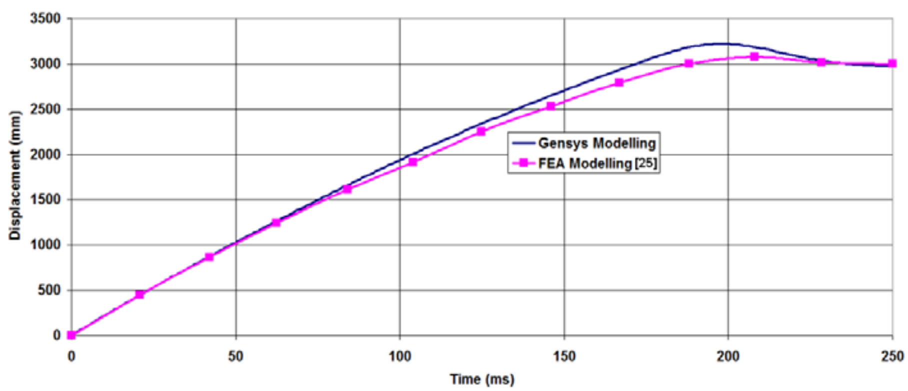

Fig. 9 Displacement Comparison

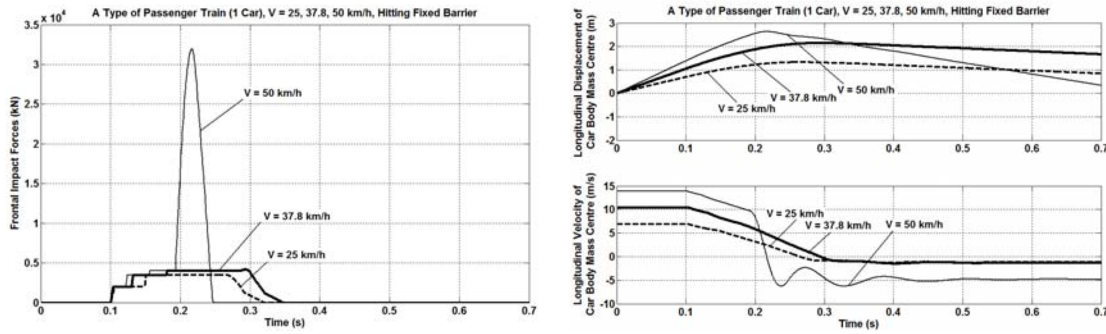

(a) Frontal Impact Forces (b) Longitudinal Displacements & Velocities

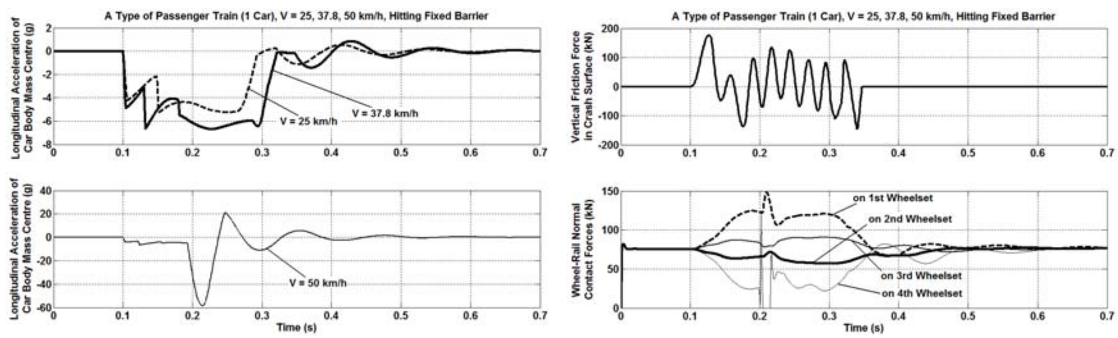

(c) Longitudinal Accelerations (d) Vertical Friction Force & Wheel-rail Forces

Fig. 10 Simulation Results

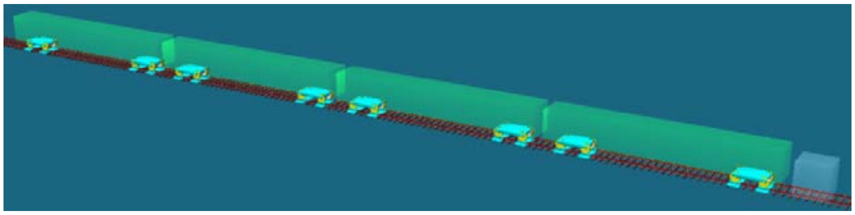

(a) Four Car Model

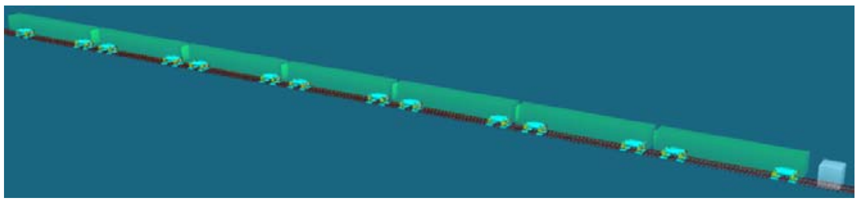

(b) Seven Car Model

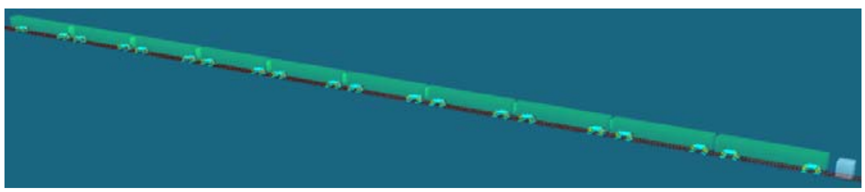

(c) Ten Car Model

Fig. 11 Train Models

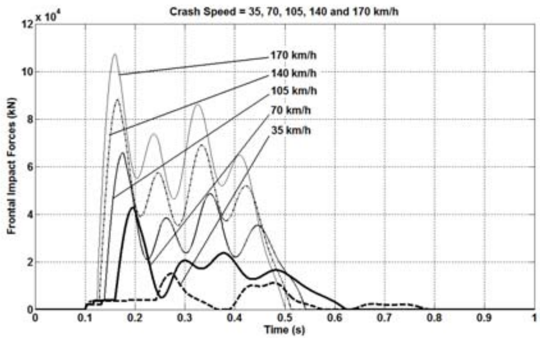

(a) Frontal impact forces

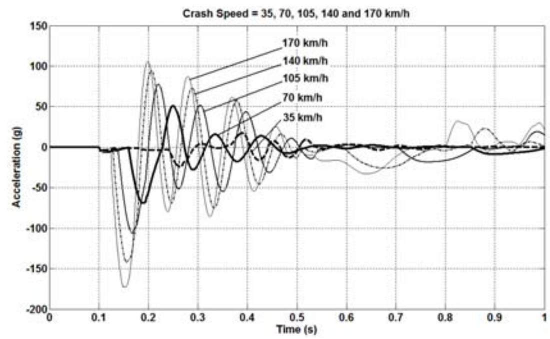

(b) accelerations at 1st car body mass centre

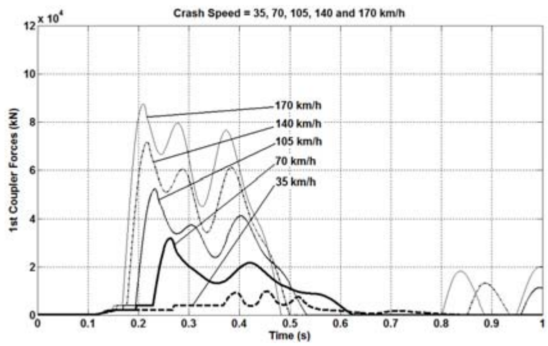

(c) First coupler forces

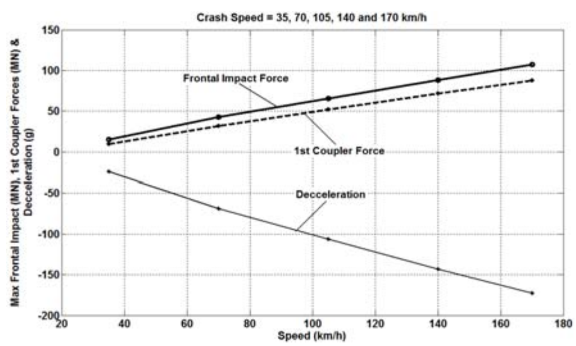

(d) Absolute maximum values verse speeds

Fig. 12 Some Simulation Results

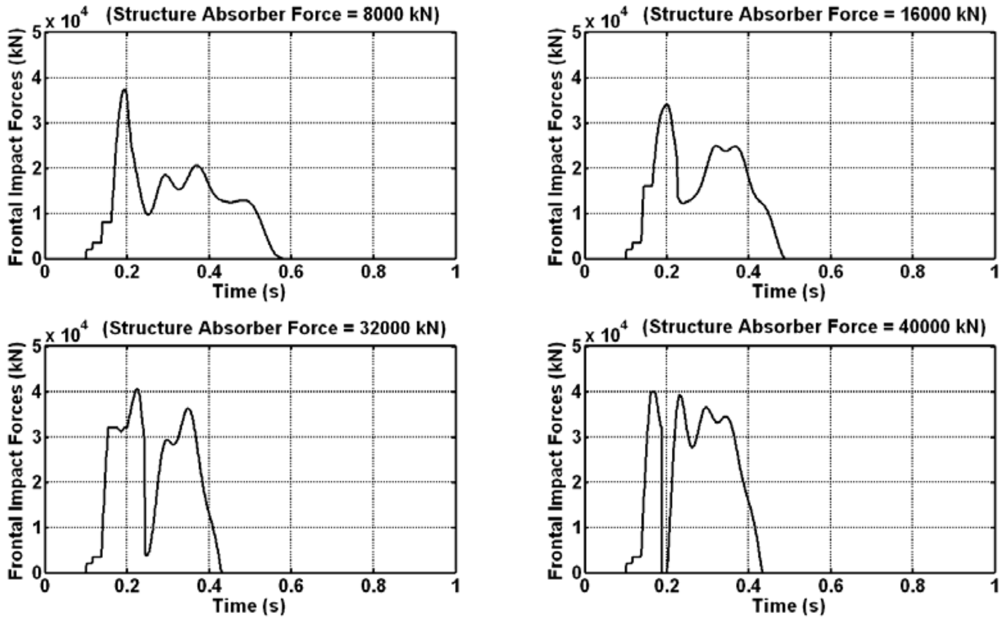

(a) Frontal Impact Forces

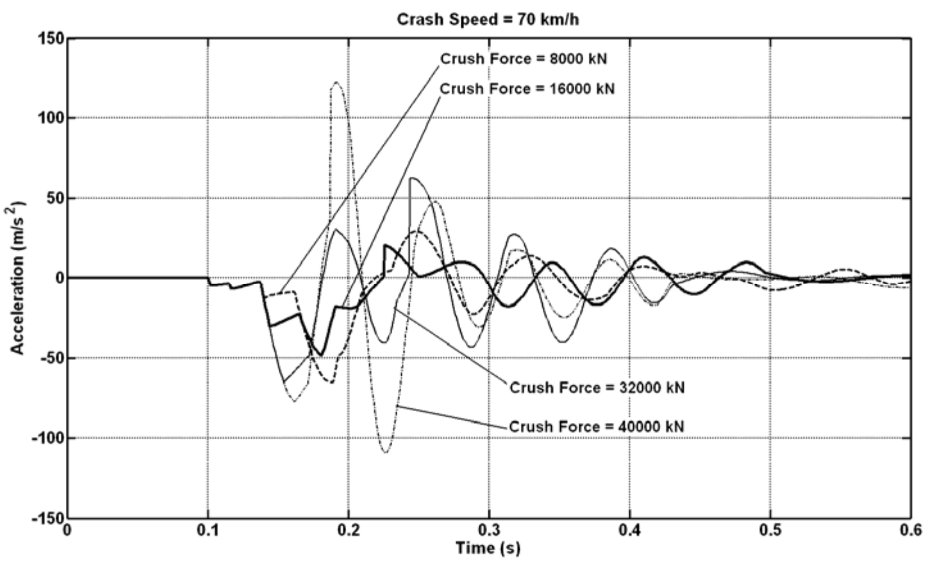

(b) Accelerations of First Car Body Mass Centre

Fig. 13 Crush Forces At Speed of 70 km/h

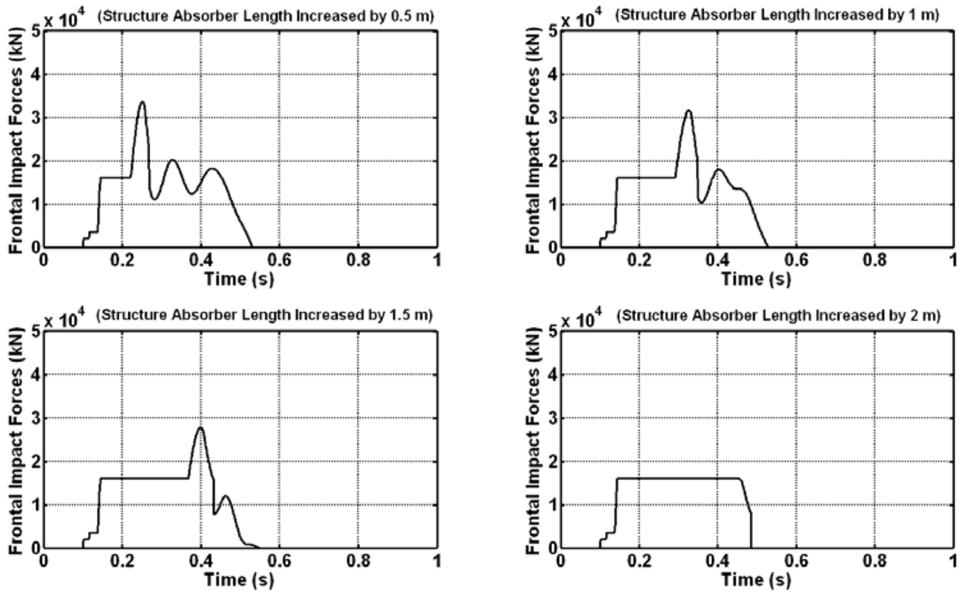

(a) Frontal Impact Forces

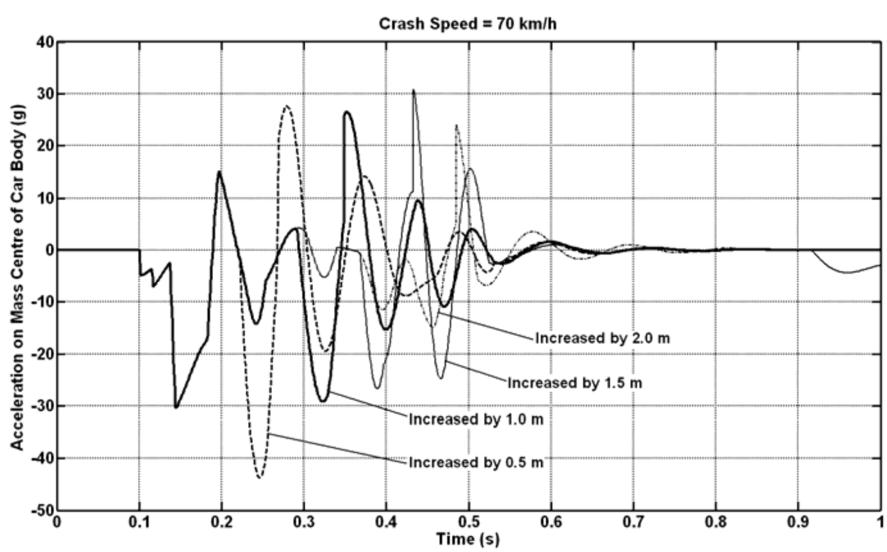

(b) Accelerations of First Car Body Mass Centre

Fig. 14 Crush Lengths At Speed of 70 km/h

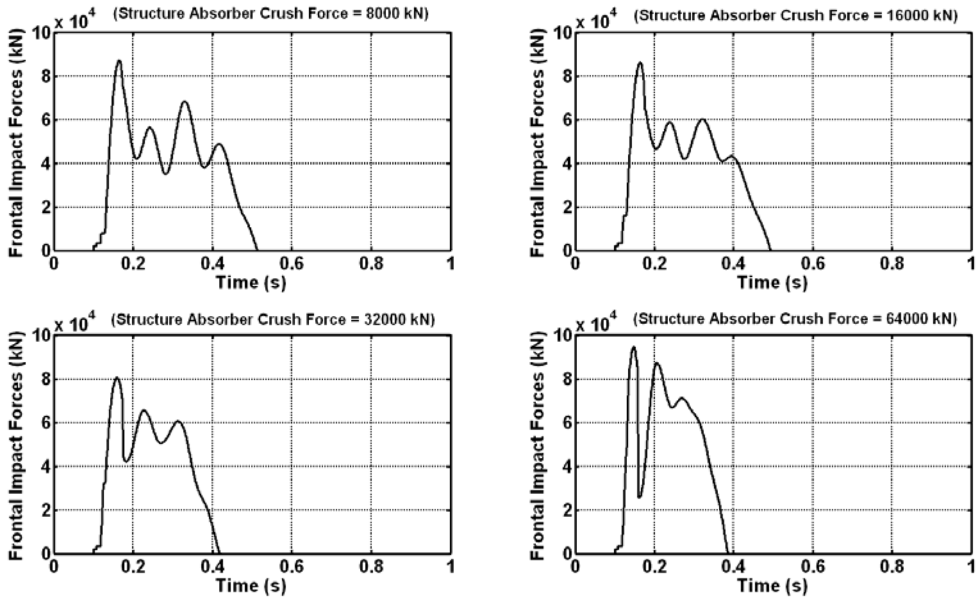

(a) Frontal Impact Forces due to Crush Forces

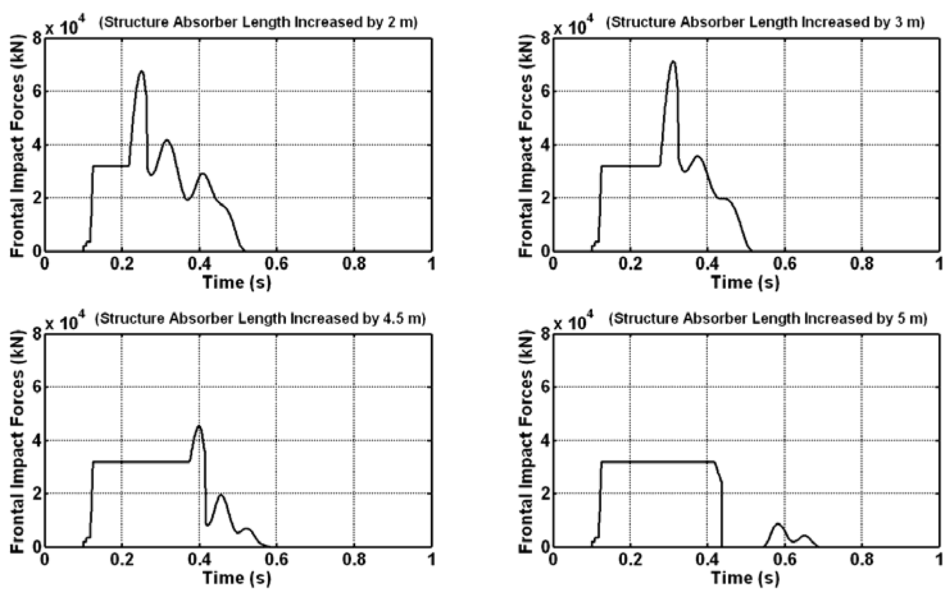

(b) Frontal Impact Forces due to Crush Length

Fig. 15 At Speed of 140 km/h

Table 1

Component	Car Body	Bogie Frame	Wheelset
Mass (kg)	40,000	6,390	1,895

Appendix – I Passenger Car Basic Parameters

Parameter		
Mass		
Wheelset	1.895	tonnes
Bolster/Spreader Beam Mass	0.8	tonnes
Bogie Mass (total including wheelset and bolster/spreader beam)	10.18	tonnes
Total Vehicle Mass (Tare)	61.7	tonnes
Seated Capacity	96	#
Loaded Mass (based on 62.5kg per seated passenger)	67.7	tonnes
Est. Gross Mass (crush load with seated and standing passengers)	71	tonnes
Suspension Stiffness and Damping		
Primary Suspension Stiffness (4 per bogie)	1067.6	N/mm
Est. Secondary Suspension Stiffness (2 per bogie)	350	N/mm
Secondary Suspension Damping (2 per bogie) below 0.025m/s	533	kN.s/m
Secondary Suspension Damping (2 per bogie) above 0.025m/s	26.7	kN.s/m
Dimensions		
Wheel Diameter (New)	920	mm
Wheel Diameter (Condemn)	860	mm
Bogie Wheel Base	2450	mm
Bogie Centres	16160	mm
Car Length (over body)	23485	mm
Car Width (overall)	2916	mm
Car height (overall)	4383	mm